European Polymer Journal 93 (2017) 448–457

Contents lists available at ScienceDirect

European Polymer Journal

journal homepage: www.elsevier.com/locate/europolj

Benzimidazole linked arylimide based covalent organic framework as gas adsorbing and electrode materials for supercapacitor application

Arkapal Roy[a], Sanjoy Mondal[a], Arijit Halder[b], Ambar Banerjee[c], Debajyoti Ghoshal[b], Ankan Paul[c], Sudip Malik[a,*]

[a] Polymer Science Unit, Indian Association for the Cultivation of Science, 2A & 2B Raja S.C Mullick Road, Jadavpur, Kolkata 700032, India
[b] Department of Chemistry, Jadavpur University, Jadavpur, Kolkata 700032, India
[c] Raman Centre for Atomic, Molecular and Optical Sciences, Indian Association for the Cultivation of Science, 2A & 2B Raja S.C. Mullick Road, Jadavpur, Kolkata 700032, India

ARTICLE INFO

Keywords:
Arylimide
Benzimidazole
CO_2 adsorption
Supercapacitive property

ABSTRACT

A novel benzimidazole appended arylimide (pyromellitic, naphthalene and perylene) based covalent organic framework (COF) has been synthesized through the condensation polymerization pathway, by taking consideration of the special noncovalent interaction with carbon dioxide. Formation and chemical connectivities of these polymers were thoroughly investigated by ^{13}C NMR and FTIR studies. Presences of pores in these polymers have been primarily checked with FESEM and HRTEM observations, prior to adsorption studies. The pyromellitic diimide containing benzimidazole COF (BIBDZ) exhibit highest BET surface area, 177.095 $m^2 g^{-1}$ with pore diameter of 30–32 angstorm among the COFs reported here which is also consistent with our computational study. Naphthalene diimide and the diaminobenzidine containing COF (NIBDZ) has the highest binding affinity with CO_2 i.e. 127.87 cc g^{-1} (14.56 wt%) at 195 K, than the other two COFs. On the other side BIBDZ has showed specific capacitance value of 88.4 F g^{-1} at 0.5 A g^{-1} current density in the 1M H_3PO_4 electrolytic solution as well as remarkable retention of specific capacitance (93.61%) after 5000 galvanostatic charge discharge cycles.

1. Introduction

Synthetic materials having molecular scale porosity consist of one, two and three dimensional networks have attracted lots of recent attention such as gas storage and separation [1,2], heterogeneous catalysis [3,4], drug delivery [5,6] and energy storage [7,8] and sensors [9], etc. Covalent organic frameworks are designed with strong covalent bonds between highly ordered organic building blocks, having excellent surface area with well defined nanopores [10,11]. In recent years, tremendous interest on different COFs to develop power supply and energy storage devices like electrochemical capacitors (supercapacitors) are growing to meet the demand for applications in powering vehicles and portable electronic devices, which are capable of charging and discharging within a few seconds, and cycle life in the order of thousands of cycle. Supercapacitors are stored the energy either by the electrical double layer capacitance through ion adsorption or the pseudo-capacitance developed from fast and reversible surface redox processes at characteristics potentials. Therefore a breakthrough in electrode material holds promise for advancement in supercapacitive nature, such as activated carbons having large surface area and good electrical properties shows capacitance up to 270 F g^{-1}. Other well-behaved

* Corresponding author.
E-mail address: psusm2@iacs.res.in (S. Malik).

http://dx.doi.org/10.1016/j.eurpolymj.2017.06.028
Received 3 April 2017; Received in revised form 15 June 2017; Accepted 16 June 2017
Available online 17 June 2017

supercapacitive materials are carbon nanotubes, graphenes, aerogels and different heteroatom hybridized carbon materials exhibit capacitances of 50–370 F g^{-1}. Recent evolution of facile as well as rational design for development of supercapacitive electrode material provides large capacitance, high energy density, however, outstanding stability remains a substantial challenge. Covalent organic frameworks (COFs) with extended π- conjugation have been synthesized via easy condensation reaction between the tetracarboxylic acid containing pyromellitic diimide and the tetramine, leading to the formation of basic benzimidazole unit with C—N and C═N bonds in the porous framework. Owing to the presence of extended π-conjugation, COFs show inherent conductivity as well as the benzimidazole units enable dipolar interaction with electrolyte cations help in accumulating protons on the walls of pores, allows quick ion motion during charge-discharge processes. Also the presence of heteroatoms (B, N, O and S) on the precise locations of porous COFs enhances the redox activity for the pseudocapacitance generation of the electrode material [12]. To develop high specific capacitance, the surface area of the electrode material should be high as it needs to incorporate large number of electrolyte ions at the electrode electrolyte interface, helps in promoting electrical double layer capacitance [13]. Owing to good thermal and chemical stability of the poly-benzimidazoles provides promising application in the electronic and automotive components, structural resins, and fire resistant materials [14] (see Scheme 1).

In this study, the synthesis of a novel benzimidazole containing arylimide based covalent framework (BIBDZ) has been reported, where benzene, naphthalene and perylene containing aryl diimide have been used as N,N′-Di-(phenyl-3,5-dicarboxylic acid)-benzenetetracarboxylic acid diimide (BI), N,N′-Di-(phenyl-3,5-dicarboxylic acid)-naphthalenetetracarboxylic acid diimide (NI), N,N′-Di-(phenyl-3,5-dicarboxylic acid)-perylene-3,4:9,10-tetracarboxylic acid diimide (PI). 3,3′-diaminobenzedene (DAB) and 1,2,4,5-benzenetetraamine (TAB) as the tetramine compound and reacted with BI/NI/PI in presence of polyphosphoric acid. Due to the presence of multiple interaction sites for CO_2 to bind with benzimidazole within polymer plays a crucial role for separation from the natural gas as considerable efforts have taken to imply for the development of viable technologies for this predominant green house capture and sequestration, coming out from anthropogenic activities such as fossil fuel burning resulting huge global warming [15].

2. Experimental section

2.1. Materials & methods

Pyromellitic dianhydride, 1,4,5,8-Naphthalenetetracarboxylicdianhydride, perylene-3,4,9,10-tetracarboxylic dianhydride (PTCDA), 5-aminoisophthalic acid (5-AIPA) and polyphosphoric acid (reagent grade, 115% H_3PO_4) were purchased from Sigma Aldrich and used without further purification. N,N′-Dimethylformamide (DMF), Imidazole, Sodium Bicarbonate ($NaHCO_3$) and Hydrochloric acid (HCl, 37%) were purchased from Merck Chemicals as analytical pure reagents. 10% (W/V) $NaHCO_3$ solutions were prepared in deionised water (18 MΩ cm, Millipore Milli Q water system).

^{13}C-CPMAS NMR spectra of the insoluble polymer samples were recorded on 500 MHz Bruker DPX spectrometer at a MAS frequency of 10 kHz and all chemical shifts were quoted using the δ scale (ppm). Fourier transform infrared (FT-IR) spectrum of KBr powder-pressed pellets was obtained from PerkinElmer Spectrum 783 spectrophotometer. Thermogravimetric analysis of the polymer samples were performed using a TA SDT Q600 instrument. Powdered XRD (PXRD) analysis was done in Bruker AXS diffractometer (D8 advance) using CuKα radiation (λ = 1.54 Å), a generator voltage of 40 kV and a current of 40 mA. XPS studies were performed by using a focused monochromatized A1 Kα X-ray source (1486.8 eV) in Omicron Nano-Technology 0571 XPS instrument. Surface morphology as well as the overall morphology of the prepared porous polymer samples were characterized by FESEM (JEOL, JSM 6700F) instrument operating at 5 kV. To reduce the surface potential samples were coated with platinum for 90 s prior to SEM experiments. TEM imaging of the polymer sample carried in HRTEM (JEOL, 2010EX) instrument an accelerating voltage of 200 kV. Small amount of ethanol dispersed samples were put over a 200 mesh Cu-grid coated with a holey carbon support.

2.2. Sorption measurements

Ambient pressure volumetric gas adsorption studies was carried out with the dehydrated samples using a Quantachrome Autosorb-iQ adsorption instrument in the relative pressures range 0–1 at 77 K maintained by a liquid-nitrogen bath and at 298 K (room temperature) for N_2 and H_2 sorption whereas CO_2 sorption measurements were performed at 195 K (attained by dry ice-acetone bath) and CH_4 sorption was carried out at 298 K (room temperature). Highly pure gases (nitrogen, 99.999%; hydrogen, 99.999%; carbon dioxide, 99.95%; methane, 99.999%) were used for the adsorption measurements. The dehydrated samples were prepared at 150 °C under a 1×10^{-1} Pa vacuum for about 6 h prior to measurement of the isotherms. Then these samples were placed into the sample tube and the change of the pressure was monitored and the degree of adsorption was determined by the decrease in pressure at the equilibrium state. All operations were computer-controlled and automatic.

2.3. Electrochemical measurements

All electrochemical experiments like cyclic voltametry (CV), galvanostatic charge/discharge (GCD), electrochemical impedance spectroscopy (EIS) were studied in a CHI6087 Electrochemical Workstation (CHI, USA) using the conventional three-electrode system. Modified glassy carbon electrode (GCE, 3 mm in diameter with a surface area of 0.07 cm^2) as a working electrode, a saturated calomel electrode (SCE) as the reference electrode, Pt wire as the calomel electrode and 1M H_3PO_4 as a electrolyte solution were used. For reuse, GCE was carefully polished with 1, 0.3, 0.05 μm alumina powder and sequentially washed through water and ethanol with sonication at room temperature until a mirror finish was obtained. The specific capacitance (C_s), energy density (E) and power

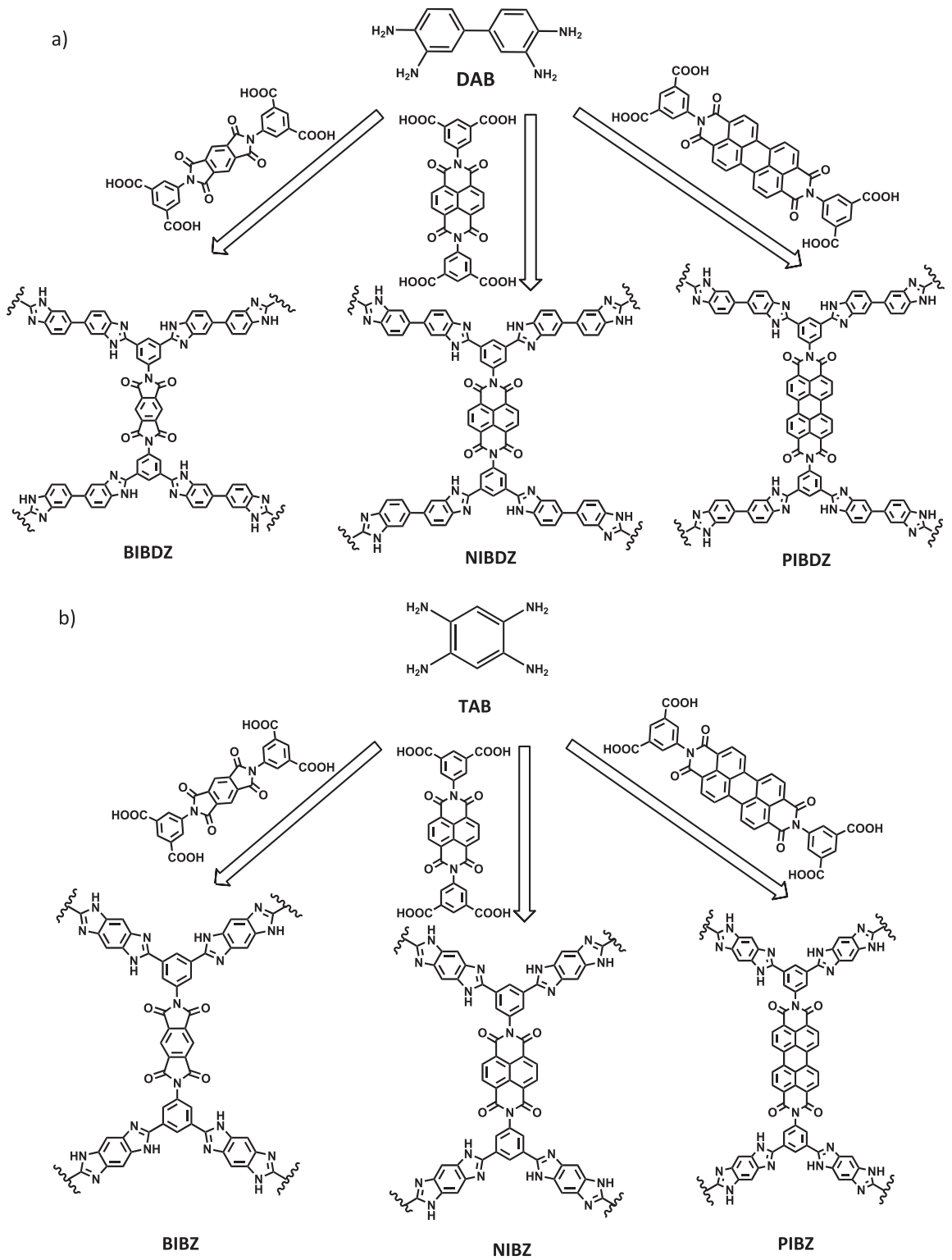

Scheme 1. Structure of the Benzimidazole linked Arylimide based porous crosslinked polymers using (a) DAB and (b) TAB.

density (P) were obtained from the discharge curve using the following three equations.

$$C_s = \frac{i \times \Delta t}{\Delta V \times m} \quad \text{(i)}$$

$$E = \frac{C_s \times \Delta V^2}{7.2} \quad \text{(ii)}$$

$$P = \frac{E \times 3600}{t} \quad \text{(iii)}$$

where i = current, m = mass of the polymer drop casted on the glossy carbon electrode surface, Δt = discharge time, ΔV = potential window [16,17].

2.4. Synthetic aspects

2.4.1. Procedure for the preparation of benzimidazole linked aryl-imide polymers

BI, NI, PI were prepared with little modified literature procedures[18,19]. Tetramine compound (2 mmol.) (DAB or TAB) was taken in 15 mL polyphosphoric acid and heated at 180 °C under inert atmosphere for 6 h, 1 mmol. of tetracarboxylic acid containing aryl-imide compound (BI, NI or PI) was mixed and further heated at 220 °C for 48 h. It was treated with 10% (W/V) $NaHCO_3$ solution, followed by filtration and dried under vacuum. In order to remove the oligomers the crude polymeric product was refluxed using Soxhlet extractor with different solvents like methanol, acetone, chloroform & DMF accordingly.

3. Results and discussion

3.1. Materials characterization

Synthesis of all benzimidazole based arylimide linked polymers was pursued through the condensation pathway between carboxylic acid and the tetramine. In the typical synthesis procedure, initially the tetramine derivatives were taken in the polyphosphoric acid under hot condition for six hours to remove the residual acid part from the tetramine molecules followed by the addition of tetracarboxylic acids (BI, NI & PI), provide the porous polymer in high yield (~85%). The chemical connectivity of those polymers were investigated by ^{13}C cross polarization/magic angle spinning (CP-MAS) NMR and FT-IR spectral analysis while chemical compositions were confirmed by microelemental analysis. As shown in Fig. 1a the carbon signal of −N−C═N− in the imidazole ring appeared at 158 ppm and the imide carbonyl carbon appeared at 168 ppm. The presence of other aromatic carbons was confirmed by multiple peaks between 120 and 150 ppm. The FT-IR spectrum (Fig. S2, ESI) contains broad bands at 3425 cm^{-1} (free N−H) and

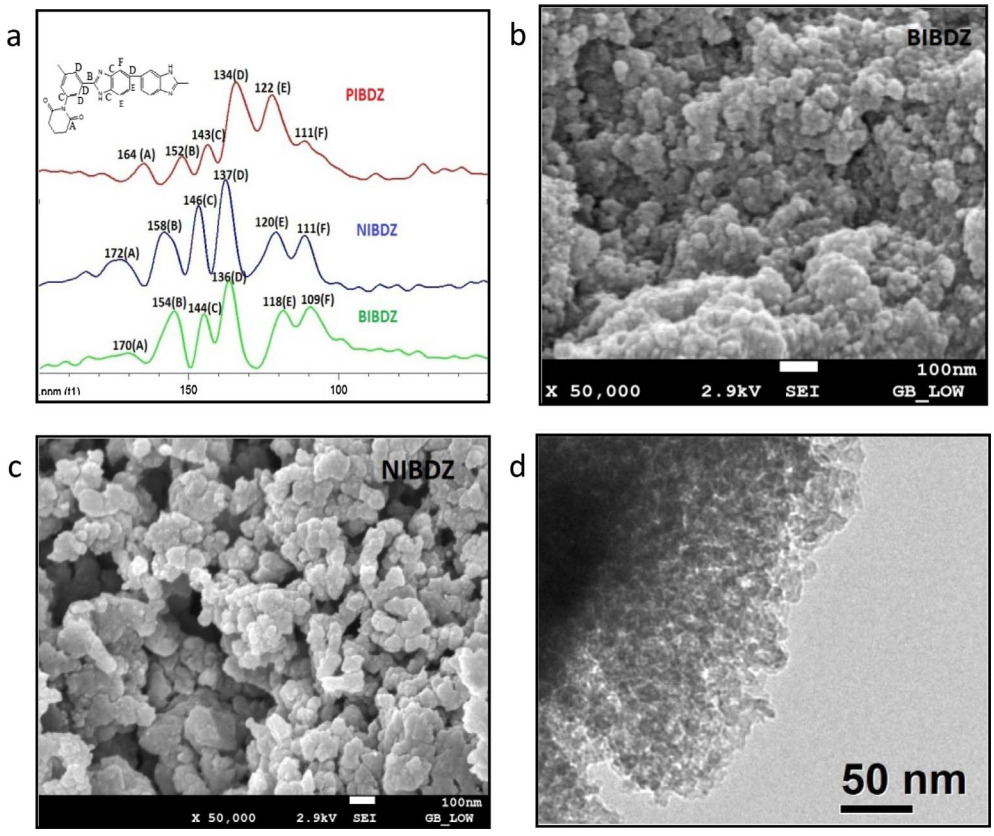

Fig. 1. (a) Solid state ^{13}C CPMAS NMR Spectra of DAB containing Polymers; (b) FESEM images of BIBDZ and (c) NIBDZ; (d) TEM image of BIBDZ.

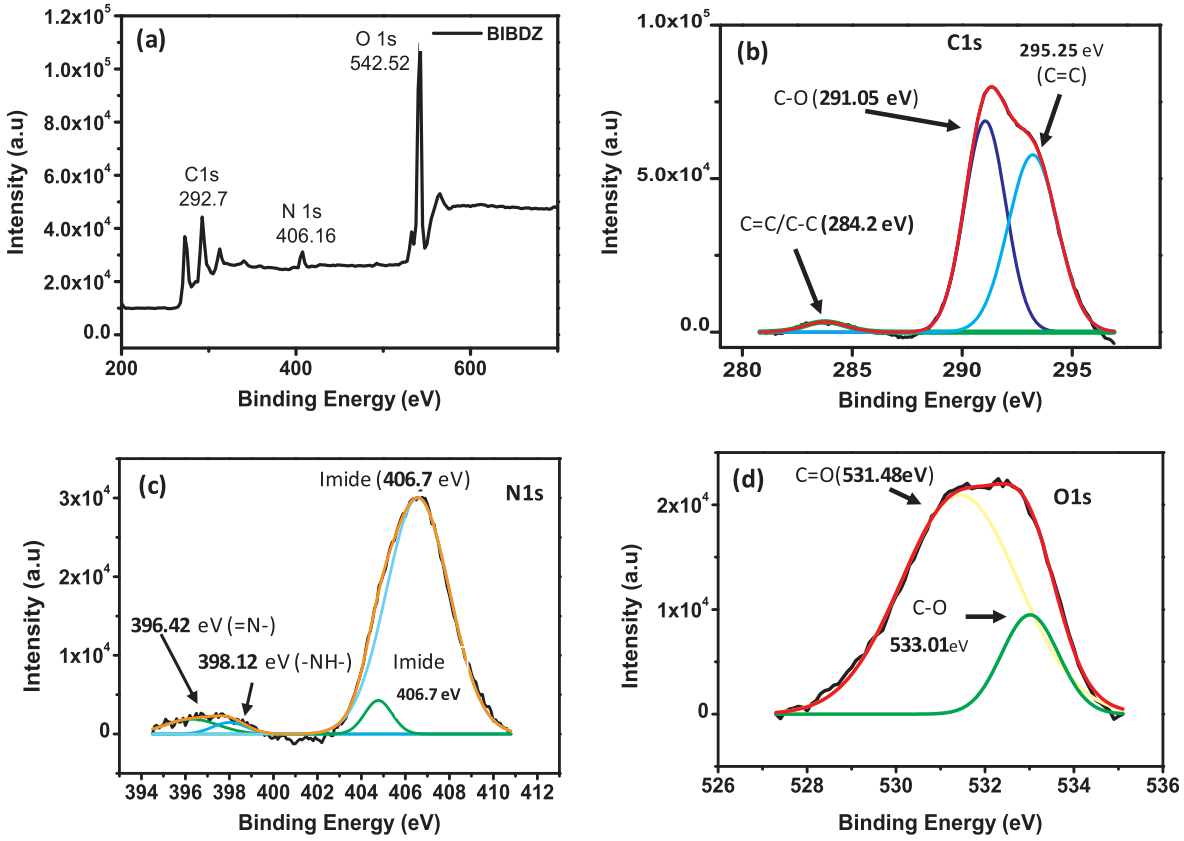

Fig. 2. XPS study of BIBDZ (a) whole scan; (b) deconvolution spectra of C1s, (c) N1 s and (d) O1s.

3235 cm^{-1} (hydrogen bonded N—H), and new bands at 1630 cm^{-1} (C═N). The absence of strong peak located at 1700 cm^{-1} indicated the full consumption of carboxylic acid group with the tetramine compound making of benzimidazole moiety. The thermal stability of the DAB attached polymers (BIBDZ, NIBDZ and PIBDZ) was checked by thermogravimetric analysis (TGA) which showed very less (< 20%) decomposition up to 400 °C (Fig. S4). The small weight losses at around 100 °C were possibly caused by the solvents remained in the porous network. Those polymers were insoluble in any common organic solvents such as dimethyl sulfoxide (DMSO), N,N′-dimethylformamide (DMF), N,N′-dimethlyacetamide (DMAc), N-methylpyrrolidone (NMP) and tetrahydrofuran (THF), reflecting the typical characteristic of hyper-cross-linked polymers. The broad peaks in the XRD patterns (Fig. S3) at 2θ = 23–24 showed that the resultant polymers were amorphous in nature. Field emission scanning electron microscopy (FE-SEM) of the polymer exhibit agglomerating morphology of small particles with rough surface and variable size (Fig. 1b and c). As well as the high resolution transmission electron microscopic (HRTEM) images (Fig. 1d) also confirmed the presence of pores. The chemical environment of the compound (BIBDZ) was further checked by XPS spectrum, where peaks at ~292.7, 406.16 and 542.52 eV assigned to C1s, N1s and O1s, respectively (Fig. 2a). The enlarge scan for C1s (Fig. 2b) of BIBDZ deconvoluted into three sub-peaks at 284.2, 291.05 & 295.25 eV for C═C/C—C, C—N/C—O & C═O respectively. The high resolution N1s spectrum (Fig. 2c) has deconvoluted into different sub-peaks at 396.42, 398.12, 404.7 & 406.7 eV, corresponding to imine, amine and imide nitrogens respectively, accompanying with the formation of the proposed COF. Pore size distribution (PSD) of BIBDZ calculated by fitting the N_2 adsorption isotherm at 77 K with non- local density functional theory (NLDFT) revealed a pore width maximum of 31 Å denoted the presence of meso pores and also the Brunauer–Emmett–Teller (BET) surface area was calculated as 177.095 m^2g^{-1} (Fig. 4a and b).

3.2. Computational study

7797803707765To further establish the porous nature of the covalent organic framework complementary semi-empirical quantum chemical investigations were conducted. Geometry optimizations were carried out to locate plausible minimum energy structures for the covalent organic frameworks. Two different semi-empirical methods, PM7 and PM6-DH2 were employed for this purpose. Both the methods contain finely tuned parameters for accurate predictions of macromolecular structure [20–22]. Organic frameworks comprising of the single, double and triple pores were optimized. All optimizations were carried out using the MOPAC 2016 semi-empirical package [23]. All the minimum energy structures for the macromolecular units exhibited the presence of large pores. Both the semi-empirical methods consistently predicted the presence of elliptical pores in the macromolecular frameworks. Hence, the major and minor radii of these pores were measured. The major and minor diameters were found to be 30.5 Å and 25.5 Å

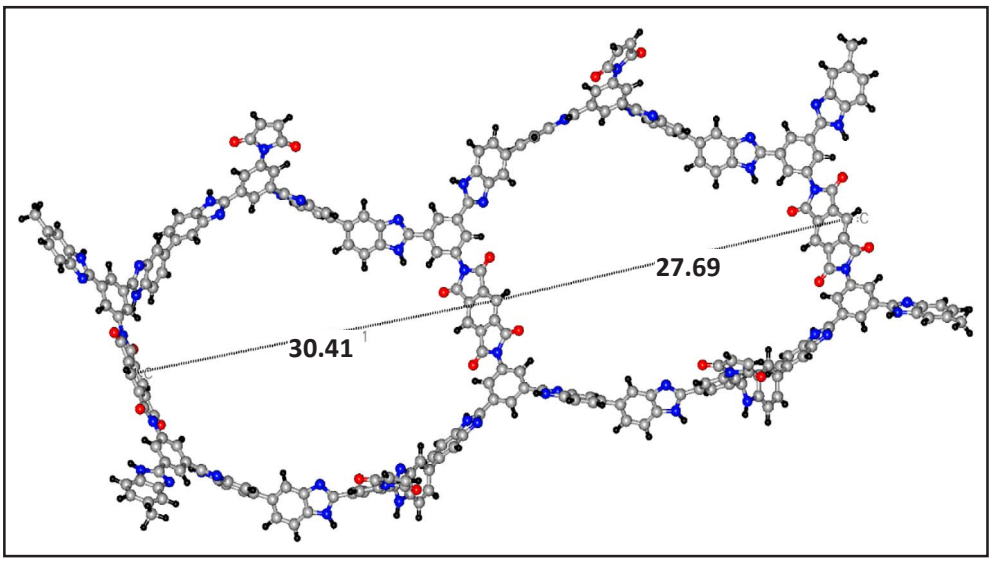

Fig. 3. Energy minimized geometry of BIBDZ calculated at the PM6-DH2 Methods. The distances are in Å. The blue, grey, black and red stands for N, C, H and O atoms, respectively. (For interpretation of the references to color in this figure legend, the reader is referred to the web version of this article.)

respectively (Fig. 3) at PM6-DH2 level of theory, which is in reasonable agreement with our experimental findings.

3.3. Porosity measurements & gas storage studies

From the structural analysis, it is evident that all of these benzimidazole containing three different arylimide polymer compounds may contain some potential pores and by activating them, a porous framework, suitable for gas adsorption might be obtained. Therefore, sorption analysis with N_2 (kinetic diameter, 3.6 Å) at 77 K resulted a typical Type IV adsorption isotherm where at low pressure little uptake of the nitrogen adsorption took place, after that a high uptake followed by a gradual uptake was observed (Fig. 4a). However, the desorption curve almost follow the adsorption curve with a slight hysteresis in some cases. In all three cases surface area was calculated from the N_2 adsorption isotherm at different relative pressure, using the BET equation. The BET consistency plot (Fig. S8) showed that BIBDZ possessed surface area (SA_{BET}) of 177.095 m^2g^{-1}, whereas that for the NIBDZ and PIBDZ, were 120 m^2g^{-1} and 75.355 m^2g^{-1} respectively. Repeated experiments taking different set of samples at identical condition show almost similar result which supports the consistency in the synthesis of the materials with respect to their surface area.

This significantly decreased surface area with increasing number of aromatic rings, is possibly explained considering the fact that the increasing π-stacking from naphthalene to perylene core was unfavourable for the pore formation due to the strong π-electron delocalization effect [24]. On the other hand polymers obtained from different tetracarboxylic acid moieties (BI, NI & PI) and TAB, namely BIBZ, NIBZ and PIBZ had very low surface area (values were given in Table. S1) which is also commensurate with their structures. The difference in surface area occurred, as the monomer DAB has one extra phenyl ring and C—C single bond compared to TAB, provides more freedom for the arrangement although both have equal side length of similar hexagonal pore. Such a freedom may leads to interpenetration or folding in case of DAB whereas the shorter and more rigid TAB monomer restricts the interpenetration of COF networks to some extent resulting in topological defects [25]. Thus for the DAB containing moieties, availability of pore is greater than the TAB containing one; causing high uptake of N_2 in their framework. To investigate about the dimension of the potentially available pores, pore size distribution (PSD) was calculated by the nonlocal density functional theory (NLDFT) through fitting of the adsorption isotherm of nitrogen measured at 77 K. The obtained value was more or less similar for all six polymers and it was in the range of 30–32 Å (Fig. 4b).

The Carbon dioxide sorption measurements have also been performed at 195 K with three DAB containing COFs having grater surface area, taking their degassed samples. It was found that NIBDZ had the maximum ability for sorption and the value was 127.87 cc g^{-1} (14.56 wt%), comparatively, the other two DAB containing polymers, PIBDZ and BIBDZ showed little less value, 119.43 cc g^{-1} (11.85 wt%) and 94.36 cc g^{-1} (11.33 wt%) respectively (Fig. 4c). These moderately high carbon dioxide affinities of the COFs may be attributed to the strong electrostatic force of interaction between the highly polar imidazole ring and the symmetric carbon dioxide molecule with a quadrupole moment, generating a dipole quadrupole interaction, (between imidazole nitrogen and the carbon atom of carbon dioxide).

Additionally there is also a complementary interaction involving aryl C—H and CO_2 (C—H——O═C═O) which may also responsible for the CO_2 selectivity of the COFs [26]. The NIBDZ showed maximum sorption 38.5 cc g^{-1} (4.02 wt%) even at room temperature (298 K) (Fig. S9). These values are quiet comparable (Table 1) with the other polybenzimidazoles measured at room temperature such as PBI-Ads [27], BILPs [28–30]. Hydrogen (77 K) and methane (298 K) sorption measurements have also been performed for NIBDZ. It has been observed that NIBDZ take a maximum amount (at 1 bar pressure) of 84.96 cc g^{-1} for hydrogen and 11.94 cc g^{-1} for methane (Fig. 4d). High value of CO_2 adsorption at 195 K as well as at room temperature provoked us to investigate

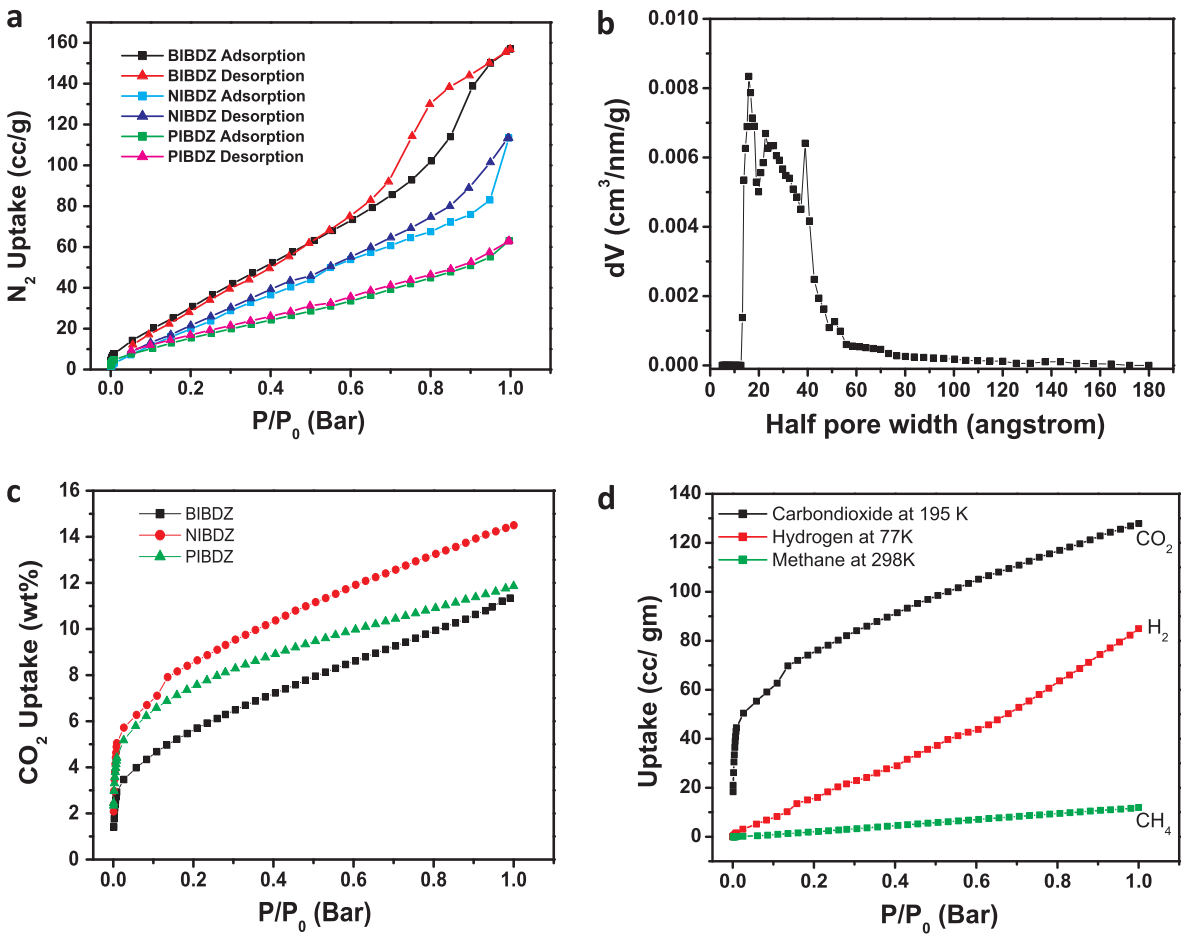

Fig. 4. (a): Adsorption (filled) and Desorption (empty) isotherms of N_2 at 77 K for BIBDZ, NIBDZ & PIBDZ at 77 K; (b) Pore size distribution of BIBDZ; (c) CO_2 adsorption isotherms of BIBDZ, NIBDZ & PIBDZ at 195 K; (d) CO_2 (195 K), H_2(77 K) and CH_4 (298 K) adsorption isotherms for BIBDZ.

the possible selectivity of NIBDZ for CO_2 over other analyte gases. For this purpose, all the gas sorption studies were performed at room temperature 298 K (Fig. S9) and initial slope was calculated for each of the adsorption isotherm. The ratios of initial slopes were calculated and that has been utilized for the estimation of the selectivity[31] of CO_2 over other. The results are quite promising and it is found that selectivity of CO_2 over N_2 is 36.9 (Fig. S10), over H_2 is 1523.3 (Fig. S11) and over CH_4 is 8.9 (Fig. S12) at room temperature.

3.4. Electrochemical measurements

The electrochemical charge storage property of BIBDZ and other COFs were analyzed with cyclic voltametry (CV) and galvanostatic charge-discharge (GCD) method with three electrode cell systems in a standard aqueous 1M H_3PO_4 solution as an electrolyte. Two reduction-oxidation peaks were observed at ~0.23 V and ~0.37 V for BIBDZ during forward (anodic) and backward (cathodic) sweep at scan rate 100 mV s^{-1} (Fig. 5a), suggesting the presence of pseudo capacitive feature along with electrical double layer capacitance. CV curves of BIBDZ (Fig. 5c) at different scan rate exhibited well resolved as well as reversible redox peaks. With increasing scan rate, peak current increased with broadening of CV peaks, signifying the pseudocapacitance nature of BIBDZ.

Table 1
Comparison of Gas adsorption properties with other benzimidazole containing Polymers.

Compounds	BET surface area (m^2 g^{-1})	Pore width (Angstrom)	Amount of adsorbed CO_2 (298 K) (at 1 bar)	Amount of adsorbed CH_4 (298 K) (at 1 bar)
BILP-2 [28]	708	6.8	52.94 cc g^{-1}	12.6 cc g^{-1}
BILP-5 [28]	599	6.8	44.29 cc g^{-1}	14 cc g^{-1}
PBI-Ad-2 [27]	926	6	~40 cc g^{-1}	–
NIBDZ (present work)	120	30.5	38.63 cc g^{-1}	12.35 cc g^{-1}

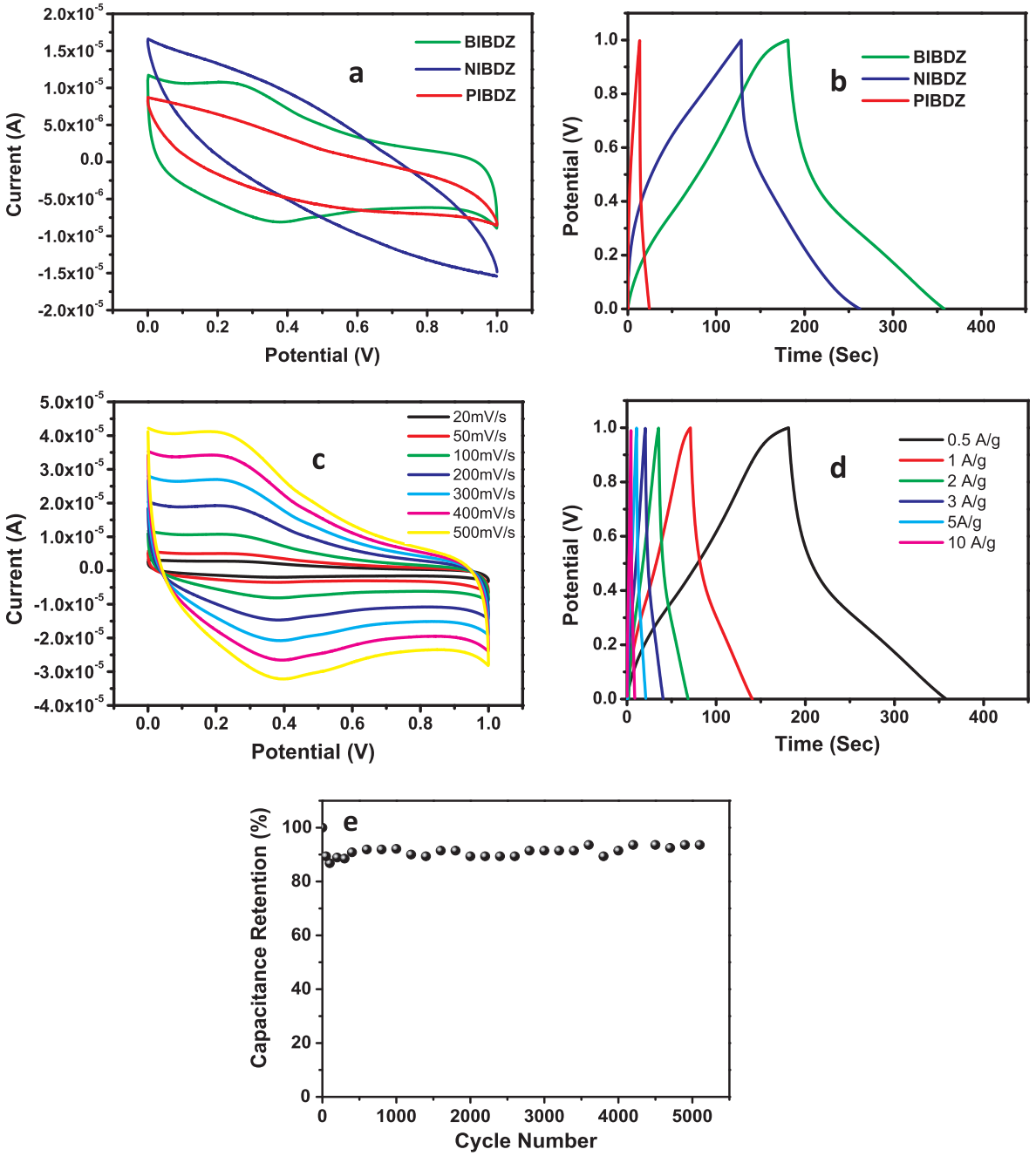

Fig. 5. (a) CV study of DAB containing Polymers at scan rate 100 mV/s in 1M H_3PO_4 solution; (b) GCD curve of the polymers at 0.5 A/g current density; (c) CV curves of BIBDZ at different scan rate; (d) GCD curve of BIBDZ at different Current density (0.5–10 A/g); (e) 3000 charge–discharge cycle life stability of BIBDZ.

Electrochemical capacitance properties of different polymers were further tested by galvanostatic charge-discharge methods at different current densities, which were of semi-triangular shape with high reversibility. Specific capacitance (C_s) was determined using the equation (*i*) from GCD curve. The measured specific capacitance values of BIBDZ, NIBDZ and PIBDZ were 88.4, 66.56 and 5.65 F g^{-1} respectively at 0.5 A g^{-1} current density (Fig. 5b). The highest capacitance (88.4 F g^{-1}) for BIBDZ resembled with highest BET surface area value in two dimensional COF morphology providing better conductive path for fast electron transport in presence of 1 M H_3PO_4 solution, which has interacting ability with the imidazole part of the COF via hydrogen bonding [32]. Also this capacitance value for BIBDZ (88.4 F g^{-1}) was compared with those of other reported carbons mentioned in Table S3 [33–35]. All GCD curves showed the nonlinear nature and also the capacitance value decreased with increasing current density. For BIBDZ, when the current density was varied from 0.5–10 A g^{-1}, the specific capacitance decreased from 88.4 F g^{-1} to 43 F g^{-1} (Fig. 5d) due to restriction of ions insertion and slow redox kinetics on electrode surface at rapid scanning. The maximum energy density (E) and the

power density (P) were 12.27 W h kg^{-1} & 249.84 W kg^{-1} respectively for BIBDZ. Long term cyclic life stability was checked with BIBDZ in the potential window 0–1 V and it was found that after 5000 continuous GCD cycle for BIBDZ, 6.39% of total specific capacitance loss occurred (i.e. 93.61% of retention of the specific capacitance) which is an indispensable parameter for the application purpose (Fig. 5e). Electrochemical impedance spectroscopy was analyzed using Nyquest plot, i.e. the plot of the imaginary part (Z″) of the impedance against the real part (Z′) and could be characterized by two distinct geometry: a semicircle at high frequency and a straight line at low frequency [36] (Fig. S15).

4. Conclusions

In conclusion, we have successfully synthesized benzimidazole linked arylimide based mesoporous polymers which have revealed gas adsorption properties as well as electrode materials utilized for energy storage. Benzidine containing tetramine (DAB) exhibited good BET surface area value than tetraminobenzene (TAB). Among the arylimides, pyromellitic moiety dominated than the other two having the π-surface of the larger Naphthalene and the perylene core, resulting in the higher BET surface area value for BIBDZ, 177.095 $m^2 g^{-1}$. Gas adsorption experiments were performed with CO_2, N_2, CH_4, H_2; and it has been found that the DAB containing COFs have better porosity in comparison to the TAB containing COFs which is in agreement with the theoretical structural elucidation. Among them NIBDZ shows selective adsorption of CO_2 at room temperature over nitrogen, hydrogen and methane. This higher surface area value for BIBDZ was also contributed well to the specific capacitance value which was around 88.4 F g^{-1} at 0.5 A g^{-1} current density, also it showed remarkable retention of specific capacitance, 93.61% after 5000 charge-discharge cycle which was thought to be the major advantage for this newly prepared benzimidazole containing COF.‘

Acknowledgement

Dr. Malik acknowledges CSIR, INDIA (project no. 02(0161)/13/EMR-II) for the partial support of this project. A. Roy thanks to CSIR, New Delhi, India for the fellowship. Dr. Ghoshal acknowledges SERB, India (project no. SB/S1/IC-06/2014) for providing the sorption facility.

Appendix A. Supplementary material

Supplementary data associated with this article can be found, in the online version, at http://dx.doi.org/10.1016/j.eurpolymj.2017.06.028.

References

[1] H.M. El-Kaderi, J.R. Hunt, J.L. Mendoza-Cortés, A.P. Côté, R.E. Taylor, M. O'Keeffe, O.M. Yaghi, Designed synthesis of 3D covalent organic frameworks, Science 316 (5822) (2007) 268–272.
[2] M.P. Suh, H.-J. Park, T.K. Prasad, D.W. Lim, Hydrogen storage in metal-organic frameworks, Chem. Rev. 112 (2) (2012) 782–835.
[3] Y. Zhang, S.N. Riduan, Functional porous organic polymers for heterogeneous catalysis, Chem. Soc. Rev. 41 (6) (2012) 2083–2094.
[4] S.Y. Ding, J. Gao, Q. Wang, Y. Zhang, W.G. Song, C.-Y. Su, W. Wang, Construction of covalent organic framework for catalysis: Pd/COF-LZU1 in Suzuki-Miyaura coupling reaction, J. Am. Chem. Soc. 133 (49) (2011) 19816–19822.
[5] H. Zhao, Z. Jin, H. Su, X. Jing, F. Sun, G. Zhu, Targeted synthesis of a 2D ordered porous organic framework for drug release, Chem. Commun. 47 (22) (2011) 6389–6391.
[6] P. Horcajada, R. Gref, T. Baati, P.K. Allan, G. Maurin, P. Couvreur, G. Ferey, R.-E. Morris, C. Serre, Metal-organic frameworks in biomedicine, Chem. Rev. 112 (2) (2012) 1232–1268.
[7] C.R. DeBlase, K.E. Silberstein, T.T. Truong, H.D. Abruña, W.R. Dichtel, β-ketoenamine-linked covalent organic frameworks capable of pseudocapacitive energy storage, J. Am. Chem. Soc. 135 (45) (2013) 16821–16824.
[8] Y.L. Wu, N.E. Horwitz, K.S. Chen, D.A. Gomez-Gualdron, N.S. Luu, L. Ma, T.C. Wang, M.-C. Hersam, J.T. Hupp, O.K. Farha, G-quadruplex organic frameworks, Nat. Chem. (in press). 10.1038/nchem.2689.
[9] S. Dalapati, S. Jin, J. Gao, Y. Xu, A. Nagai, D. Jiang, An azine-linked covalent organic framework, J. Am. Chem. Soc. 135 (46) (2013) 17310–17313.
[10] A.G. Slater, A.I. Cooper, Function-led design of new porous materials, Science 348 (6238) (2015) 6238.
[11] J.W. Colson, W.R. Dichtel, Rationally synthesized two-dimensional polymers, Nat. Chem. 5 (6) (2013) 453–465.
[12] Y.B. Huang, P. Pachfule, J.K. Sun, Q. Xu, From covalent-organic frameworks to hierarchically porous B-doped carbons: a molten-salt approach, J. Mater. Chem. A 4 (11) (2016) 4273–4279.
[13] P. Simon, Y. Gogotsi, Materials for electrochemical capacitors, Nat. Mater. 7 (11) (2008) 845–854.
[14] Y. Cui, Q.Y. Cheng, H. Wu, Z. Wei, B.-H. Han, Graphene oxide-based benzimidazole-crosslinked networks for high-performance supercapacitors, Nanoscale 5 (18) (2013) 8367–8374.
[15] R. Quadrelli, S. Peterson, Recent trends in CO_2 emissions from fuel combustion, Energy Policy 35 (11) (2007) 5938–5952.
[16] S. Mondal, U. Rana, S. Malik, Graphene quantum dot-doped polyaniline nanofiber as high performance supercapacitor electrode materials, Chem. Commun. 51 (62) (2015) 12365–12368.
[17] Y. Kou, Y. Xu, Z. Guo, D. Jiang, Supercapacitive energy storage and electric power supply using an Aza-fused π-conjugated microporous framework, Angew. Chem. Int. Ed. 50 (37) (2011) 8753–8757.
[18] T.K. Prasad, D.H. Hong, M.P. Suh, High gas sorption and metal-ion exchange of microporous metal-organic frameworks with incorporated imide groups, Chem. Eur. J. 16 (47) (2010) 14043–14050.
[19] P.K. Sukul, D. Asthana, P. Mukhopadhyay, D. Summa, L. Muccioli, C. Zannoni, D. Beljonne, A.E. Rowan, S. Malik, Assemblies of perylene diimide derivatives with melamine into luminescent hydrogels, Chem. Commun. 47 (43) (2011) 11858–11860.
[20] J. Řezáč, J. Fanfrlík, D. Salahub, P. Hobza, Semiempirical quantum chemical PM6 method augmented by dispersion and H-bonding correction terms reliably describes various types of noncovalent complexes, J. Chem. Theory Comput. 5 (7) (2009) 1749–1760.
[21] M. Korth, M. Pitonak, J. Rezac, P. Hobza, Transferable H-bonding correction for semiempirical quantum-chemical methods, J. Chem. Theory Comput. 6 (1) (2010) 344–352.
[22] J. Hostaš, J. Řezáč, P. Hobza, On the performance of the semiempirical quantum mechanical PM6 and PM7 methods for noncovalent interactions, Chem. Phys.

Lett. 568 (2013) 161–166.
[23] MOPAC2016, James J.P. Stewart, Stewart Computational Chemistry, Colorado Springs, CO, USA, 2016. < http://OpenMOPAC.net > .
[24] Z. Wang, B. Zhang, H. Yu, L. Sun, C. Jiao, W. Liu, Microporous polyimide networks with large surface areas and their hydrogen storage properties, Chem. Commun. 46 (41) (2010) 7730–7732.
[25] H. Yu, C. Shen, Z. Wang, Micro- and mesoporous polycyanurate networks based on triangular units, ChemPlusChem 78 (6) (2013) 498–505.
[26] S. Altarawneh, S. Behera, P. Jena, H.-M. El-Kaderi, New insights into carbon dioxide interactions with benzimidazole-linked polymers, Chem. Commun. 50 (27) (2014) 3571–3574.
[27] B. Zhang, G. Li, J. Yan, Z. Wang, Tetraphenyladamantane-based microporous polybenzimidazoles for adsorption of carbon dioxide, hydrogen, and organic vapors, J. Phys. Chem. C 119 (2015) 13080–13087.
[28] M.G. Rabbani, H.M. El-Kaderi, Synthesis and characterization of porous benzimidazole-linked polymers and their performance in small gas storage and selective uptake, Chem. Mater. 24 (8) (2012) 1511–1517.
[29] M.G. Rabbani, H.M. El-Kaderi, Template-free synthesis of a highly porous benzimidazole-linked polymer for CO_2 capture and H_2 storage, Chem. Mater. 23 (7) (2011) 1650–1653.
[30] M.G. Rabbani, T.E. Reich, R.-M. Kassab, K.T. Jackson, H.M. El-Kaderi, High CO_2 uptake and selectivity by triptycene-derived benzimidazole-linked polymers, Chem. Commun. 48 (8) (2012) 1141–1143.
[31] D.K. Maity, A. Halder, B. Bhattacharya, A. Das, D. Ghoshal, Selective CO_2 adsorption by nitro functionalized metal organic frameworks, Cryst. Growth Des. 16 (3) (2016) 1162–1167.
[32] A. Sannigrahi, S. Ghosh, S. Maity, T. Jana, Polybenzimidazole gel membrane for the use in fuel cell, Polymer 52 (19) (2011) 4319–4330.
[33] J.H. Lee, W.H. Shin, M.H. Ryou, J.K. Jin, J. Kim, J.W. Choi, Functionalized graphene for high performance lithium ion capacitors, ChemSusChem 5 (12) (2012) 2328–2333.
[34] C. Portet, P.L. Taberna, P. Simon, E. Flahaut, C. Laberty-Robert, High power density electrodes for carbon supercapacitor applications, Electrochim. Acta 50 (20) (2005) 4174–4181.
[35] A. Balducci, R. Dugas, P.L. Taberna, P. Simon, D. Plee, M. Mastragostino, S. Passerini, High temperature carbon–carbon supercapacitor using ionic liquid as electrolyte, J. Power Sources 165 (2) (2007) 922–927.
[36] G. Wang, L. Zhang, J. Zhang, A review of electrode materials for electrochemical supercapacitors, Chem. Soc. Rev. 41 (2) (2012) 797–828.